

Contents lists available at [ScienceDirect](http://ScienceDirect.com)

Physics Letters B

www.elsevier.com/locate/physletbMeasurement of the neutron-capture cross section of ^{76}Ge and ^{74}Ge below 15 MeV and its relevance to $0\nu\beta\beta$ decay searches of ^{76}Ge Megha Bhike^{a,b,*}, B. Fallin^{a,b}, Krishichayan^{a,b}, W. Tornow^{a,b}^a Department of Physics, Duke University, Durham, NC 27708, USA^b Triangle Universities Nuclear Laboratory, Durham, NC 27708, USA

ARTICLE INFO

Article history:

Received 1 September 2014

Received in revised form 2 December 2014

Accepted 3 December 2014

Available online 9 December 2014

Editor: D.F. Geesaman

Keywords:

Neutron radiative capture

Neutron induced background

Neutrino detectors

Double-beta decay detectors

Dark matter detectors

ABSTRACT

The neutron radiative-capture cross section of ^{76}Ge was measured between 0.4 and 14.8 MeV using the activation technique. Germanium samples with the isotopic abundance of $\sim 86\%$ ^{76}Ge and $\sim 14\%$ ^{74}Ge used in the $0\nu\beta\beta$ searches by the GERDA and Majorana Collaborations were irradiated with monoenergetic neutrons produced at eleven energies via the $^3\text{H}(p, n)^3\text{He}$, $^2\text{H}(d, n)^3\text{He}$ and $^3\text{H}(d, n)^4\text{He}$ reactions. Previously, data existed only at thermal energies and at 14 MeV. As a by-product, capture cross-section data were also obtained for ^{74}Ge at neutron energies below 8 MeV. Indium and gold foils were irradiated simultaneously for neutron fluence determination. High-resolution γ -ray spectroscopy was used to determine the γ -ray activity of the daughter nuclei of interest. For the ^{76}Ge total capture cross section the present data are in good agreement with the TENDL-2013 model calculations and the ENDF/B-VII.1 evaluations, while for the $^{74}\text{Ge}(n, \gamma)^{75}\text{Ge}$ reaction, the present data are about a factor of two larger than predicted. It was found that the $^{74}\text{Ge}(n, \gamma)^{75}\text{Ge}$ yield in the High-Purity Germanium (HPGe) detectors used by the GERDA and Majorana Collaborations is only about a factor of two smaller than the $^{76}\text{Ge}(n, \gamma)^{77}\text{Ge}$ yield due to the larger cross section of the former reaction.

© 2014 The Authors. Published by Elsevier B.V. This is an open access article under the CC BY license (<http://creativecommons.org/licenses/by/3.0/>). Funded by SCOAP³.

1. Introduction

The physics motivations for searches of neutrino-less double-beta decay ($0\nu\beta\beta$) are well known [1]. Currently, large scale searches are underway using the target isotopes ^{76}Ge [2,3], ^{130}Te [4] and ^{136}Xe [5,6], while a number of other double-beta decay isotopes are used in smaller-scale experiments. It is interesting to point out that in most ongoing or planned experiments the double-beta decay target isotope is also the main component of the detector material. The most notable exceptions are KamLAND-Zen [6], NEMO [7], and SNO+ [8]. Common to all $0\nu\beta\beta$ decay searches is the requirement that background events in the energy region of interest, a narrow energy band centered at the Q-value for $0\nu\beta\beta$, must be extremely small. The typical goal is one count per keV, per tonne of target material and year of counting. To put this goal in perspective, we note that the current value published recently by the GERDA Collaboration is 10 counts $\text{keV}^{-1} \text{t}^{-1} \text{yr}^{-1}$ [2]. However, for covering the inverted

neutrino-mass hierarchy region, an even lower background limit than 1 count $\text{keV}^{-1} \text{t}^{-1} \text{yr}^{-1}$ is required. Approaching such a low level of background requires not only extremely radio-pure target and shielding materials to minimize internal radiation, but also sophisticated measures to minimize external radiation, especially cosmic-ray or (α, n) produced neutrons, which in turn have the potential to contribute to the internal radiation in the γ -ray energy region of interest.

Although the neutron slowing-down process is complicated, cosmic-ray produced spallation neutrons with energies above 10 MeV tend to undergo the $^A\text{X}(n, 2n)^{A-1}\text{X}$ reaction, which by far has the largest cross section (1 to 2 b) of all possible reaction channels and which peaks at approximately 15 to 20 MeV incident neutron energy. This process not only increases the neutron flux by a factor of two, but also may result in radioactive daughter nuclei ^{A-1}X , in addition to the de-excitation γ rays before the ^{A-1}X nucleus reaches its ground state. Eventually, most of the neutrons will be captured via the radiative-capture reaction $^A\text{X}(n, \gamma)^{A+1}\text{X}$, resulting in a cascade of prompt de-excitation γ rays from excited states of the ^{A+1}X nucleus with excitation energies of typically 6 to 7 MeV for thermal neutron capture, and delayed γ rays, if the ^{A+1}X nucleus is radioactive. Although the thermal neutron-capture cross section is known to be considerably larger than

* Corresponding author at: Department of Physics, Duke University, Durham, NC 27708, USA.

E-mail address: megha@tunl.duke.edu (M. Bhike).

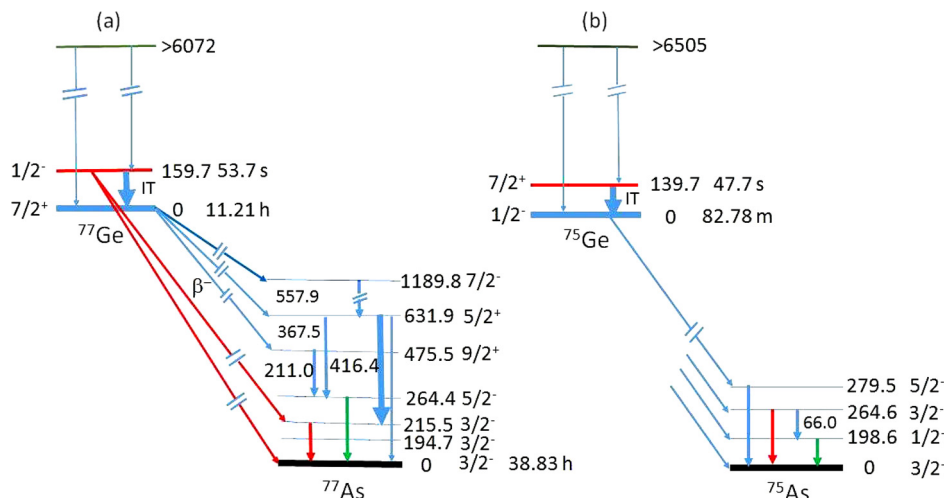


Fig. 1. (Color online.) Partial level schemes of interest for (a) the $^{76}\text{Ge}(n, \gamma)$, and (b) $^{74}\text{Ge}(n, \gamma)$ reactions. All energies are in keV. The excitation energies of 6072 keV and 6505 keV refer to thermal neutron capture on ^{76}Ge and ^{74}Ge .

the neutron-capture cross section at MeV energies, neutron capture reactions can occur before thermalization, resulting in higher excitation energies of the nucleus ^{A+1}X . In addition, angular momentum values $l > 0$ can be transferred. Both effects provide for a richer de-excitation γ -ray spectrum than obtained with thermal neutrons. For (α, n) neutrons the $^A\text{X}(n, 2n)^{A-1}\text{X}$ channel is typically not open, and therefore, these neutrons will basically undergo the radiative capture process only, because the other open reaction channels have only very small cross sections.

In order to more accurately predict the neutron-induced internal background in the ^{76}Ge based $0\nu\beta\beta$ decay searches GERDA and Majorana, the neutron-capture cross section of ^{76}Ge and ^{74}Ge must be known. In these two experiments enriched High-Purity Germanium (HPGe) is used as target and detector material with isotopic abundance of approximately 86% ^{76}Ge and 14% ^{74}Ge . For ^{76}Ge the neutron-capture cross section has been measured previously only at thermal energies and at 14 MeV, while for ^{74}Ge data exist up to 4 MeV.

Simplified decay schemes for ^{77}Ge and ^{75}Ge are given in Fig. 1. As can be seen, prompt γ rays with total energies of above 6072 keV (from the de-excitation of ^{77}Ge) and 6505 keV (from the de-excitation of ^{75}Ge) are emitted before beta decay to ^{77}As (for ^{77}Ge) and ^{75}As (for ^{75}Ge) takes place. The ground-state half-life times of ^{77}Ge with spin/parity $7/2^+$ and ^{75}Ge with spin/parity $1/2^-$ are 11.2 h and 82.8 m, respectively. These times are long compared to the half-life times of the isomeric transitions (IT) $1/2^- \rightarrow 7/2^+$ in ^{77}Ge and $7/2^+ \rightarrow 1/2^-$ in ^{75}Ge of 53.7 s and 47.7 s, respectively. Both IT transitions feed the associated ground state. The isomeric state of ^{77}Ge β^- decays with a sizable branching ratio (19%). Therefore, in order to obtain the total capture cross section, its decay to ^{77}As has to be considered, in addition to the ground state β^- decay of ^{77}Ge . Because of the short half-life of the 159.7 keV state of only 53.7 s, measuring its decay provides an experimental challenge due to the lack of sufficiently intense monoenergetic neutron sources in the MeV energy range. The β^- -decay branching ratio of the 139.7 keV isomeric state of ^{75}Ge is only 0.030%, and therefore, will be neglected in the following.

There are no levels known to exist in ^{77}Ge and ^{75}Ge and their daughters ^{77}As and ^{75}As , respectively, which produce a single γ ray in the vicinity of 2039 keV, the $0\nu\beta\beta$ decay Q-value of ^{76}Ge . The 2037.87 keV γ ray resulting from the decay of the 2513.47 keV level in ^{77}As is either in coincidence with a 475.48 keV γ ray or with two γ rays of 264.43 keV and 211.03 keV, making it less

likely to be detected as a 2037.87 keV single-site event. However, the very recent work of Toh et al. [9] on ^{76}Ge clearly showed that the level scheme of ^{76}Ge , as given in NNDC [10], is incomplete. Therefore, most likely, the same holds for the nuclei of interest to the present work. Independent of this conjecture, the decay of levels with energies above 2300 keV could produce Compton scattered γ rays with the single-site event signature characteristic for $0\nu\beta\beta$ decay, if the remaining energy is not recorded in the detector or cannot be used as a veto condition.

Recently, accurate neutron radiative-capture cross-section data were published by Meierhofer et al. [11,12] at thermal energies for both ^{76}Ge and ^{74}Ge . Their results for the total thermal capture cross section σ_t are 68.8 ± 3.4 mb for ^{76}Ge and 497 ± 52 mb for ^{74}Ge . These values agree with previous, but less accurate measurements [13–18]. Given the abundance ratio of 0.16 for ^{74}Ge to ^{76}Ge in the HPGe detectors used by both the GERDA and Majorana Collaborations, it is of interest to note that the potential γ -ray background originating from thermal neutron capture on ^{74}Ge is almost as important as that on ^{76}Ge .

In the present work we present data for the neutron radiative-capture cross section of ^{76}Ge obtained at 11 energies in the neutron energy range between 0.4 and 14.8 MeV and at 10 energies for ^{74}Ge below 8 MeV.

2. Experimental setup and procedure for germanium irradiation

Metallic germanium targets of 10 mm \times 10 mm area and thickness of 2 mm (resulting in about 1.5 g) were used. The isotopic composition is the same as that of the enriched HPGe detectors used by the GERDA and Majorana Collaborations. For neutron fluence determination the germanium slab was sandwiched between either indium or gold foils of the same area and thickness of 0.125 mm and 0.01 mm, respectively. The slab was supported by a thin plastic foil and was positioned at a distance of 10 mm from the end of the neutron production target. The entire assembly was surrounded by a cage made of 0.5 mm thick cadmium. The cadmium cage effectively prevented room-return thermal neutrons from interacting with the target assembly. Fig. 2 shows a schematic view of the arrangement used for neutron energies between 4.39 and 7.36 MeV. In this energy range neutrons were produced via the $^2\text{H}(d, n)^3\text{He}$ reaction, employing a deuterium gas cell pressurized to 3 atm of high-purity deuterium gas. The neutron flux on target was typically $5 \times 10^7 \text{ s}^{-1} \text{ cm}^{-2}$ for incident deuteron currents of up to 2 μA . For neutron energies between 0.4 MeV and

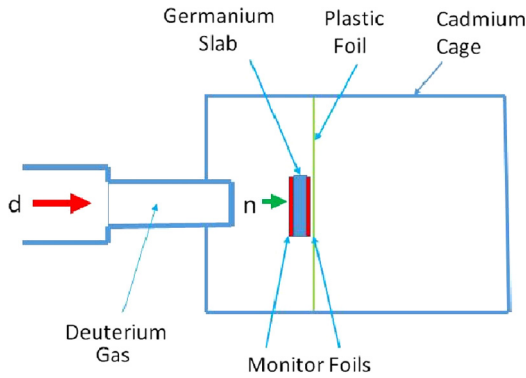


Fig. 2. (Color online.) Schematic of the experimental setup used for the $^{74,76}\text{Ge}(n, \gamma)^{75,77}\text{Ge}$ measurements using the $^2\text{H}(d, n)^3\text{He}$ reaction.

Table 1
Relevant data for Ge isotopes [10].

Isotope	Half-life	γ -ray energy (keV)	γ -ray intensity (%)
^{75}Ge	82.78(4) m	264.6(1)	11.4
		198.6(1)	1.19(12)
^{75m}Ge	47.7(5) s	139.68(3)	39.51
^{77}Ge	11.211(3) h	264.450(25)	53.3
		211.03(4)	30.0(8)
		215.51(4)	27.9(7)
		416.35(4)	22.7(11)
		367.49(4)	14.5(7)
^{77m}Ge	53.7(6) s	159.7(1)	10.3(11)

3.39 MeV the $^3\text{H}(p, n)^3\text{He}$ reaction was used, featuring the tritiated titanium target described in Ref. [19]. In this case the neutron flux was about one order of magnitude lower. The same tritiated target was employed with an incident deuteron beam to produce 14.81 MeV neutrons by means of the $^3\text{H}(d, n)^4\text{He}$ reaction. Here, the neutron flux was typically $2.8 \times 10^7 \text{ s}^{-1} \text{ cm}^{-2}$. Because our germanium target contains both ^{74}Ge and ^{76}Ge , it was impossible to obtain neutron capture data on ^{74}Ge at 14.81 MeV with our experimental method, because the daughter nucleus ^{75}Ge is the same as that of the $^{76}\text{Ge}(n, 2n)^{75}\text{Ge}$ reaction, which has a three orders of magnitude larger cross section than the $^{74}\text{Ge}(n, \gamma)^{75}\text{Ge}$ reaction. The former has a reaction threshold of 9.55 MeV.

Neutron irradiation times were typically 4 hours for measuring the ground-state decay of ^{77}Ge and ^{75}Ge . After irradiation, the germanium slab and the monitor foils were γ -ray counted with calibrated and well-shielded High-Purity Germanium detectors of known efficiency. Unfortunately, the 264.45 keV transition, the most intense γ -ray line emitted by ^{77}As , has practically the same energy as the 264.6 keV transition, the strongest γ -ray line emitted by ^{75}As (see Fig. 1 and Table 1). Although the associated half-life times are very different, and therefore, would allow in principle for the individual determination of the two γ -ray intensities, we used the 211.1, 416.35 and 367.49 keV γ rays for the activity determination of ^{77}Ge . Good agreement was found between these alternative transitions. The 215.5 keV state in ^{77}As is populated via β^- decay from both the isomeric and ground state of ^{77}Ge . Therefore, the associated strong decay is only useful for our purposes after a waiting time of about 10 minutes.

Because the isomeric 159.7 keV state with $T_{1/2} = 53.7$ s contributes to σ_t , its contribution is needed to determine the direct ground-state decay cross section σ_d of ^{77}Ge from the relation $\sigma_d = \sigma_t - 0.19 \times \sigma_m$, where 0.19 ± 0.02 is the branching of the isomeric state to the ground state, and σ_m is the $^{76}\text{Ge}(n, \gamma)^{77m}\text{Ge}$ cross section to the isomeric state.

Table 2
Relevant data for monitor reactions [10].

Reaction	Half-life	γ -ray energy (keV)	γ -ray intensity (%)
(a) $^{115}\text{In}(n, n')^{115m}\text{In}$	4.486(4) h	336.241(25)	45.8(22)
(b) $^{115}\text{In}(n, \gamma)^{116m1}\text{In}$	54.29(17) m	1293.56(2)	84.8(12)
(c) $^{197}\text{Au}(n, 2n)^{196}\text{Au}$	6.1669(6) d	355.73(5)	87

In order to measure σ_m , the neutron irradiation time was limited to 3 min to avoid saturation. The induced low activity in the germanium slab and associated monitor foils compared to the 4 h irradiation time used for the measurements of the ground-state capture cross section, unavoidably resulted in larger uncertainties. To partially compensate for this deficiency, up to six individual irradiations were performed at each energy.

3. Analysis and results

The activation formula [20] was used to determine the neutron flux from the monitor reactions. Table 2 provides information on the γ -ray energies and their uncertainties. The second column of Table 3 gives the cross-section values σ_{mon} used for the monitor reactions at the neutron energies of interest. Monte-Carlo calculations were performed to obtain the mean neutron energy and its associated energy spread. The differential cross-section data for the neutron production reactions were taken from Refs. [21,22]. The same Monte-Carlo code was used to account for the tight geometry of the experimental setup which causes the average of the neutron fluences deduced from the two monitor foils to deviate slightly from the neutron fluence seen by the germanium slab. The activation formula was also employed to obtain σ_t and σ_m from the measured activities, as described in [20]. Results are given in columns 3, 4 and 5 of Table 3 for σ_t , σ_m , and σ_d for the reaction $^{76}\text{Ge}(n, \gamma)^{77}\text{Ge}$, $^{76}\text{Ge}(n, \gamma)^{77m}\text{Ge}$, and $^{76}\text{Ge}(n, \gamma)^{77d}\text{Ge}$, respectively. Table 4 summarizes the uncertainty budget. Fig. 3 shows our data for σ_t in comparison to the previous datum of Begun et al. [26] at 13.96 MeV and the results of the evaluations ENDF/B-VII.1 [27] and CENDL-3.1 [29], and the model calculation TENDL-2013 [30]. Considering that these predictions relied only on the 13.96 MeV datum, there is surprisingly good agreement between our data and ENDF/B-VII.1 and TENDL-2013 in the energy region of interest.

Fig. 4 and column 4 of Table 3 present our cross-section data σ_m for the capture to the isomeric state of ^{77}Ge . This cross section is as large as the direct one to the ground state of ^{77}Ge (see column 5 of Table 3).

As stated earlier, cross-section information for the $^{74}\text{Ge}(n, \gamma)^{75}\text{Ge}$ reaction was obtained as well. Here, the weak 198.6 keV transition (see Fig. 1 and Table 1) was used. The capture to the 139.7 keV state of ^{75}Ge with $T_{1/2} = 47.7$ s was measured simultaneously with the capture to the 159.7 keV state of ^{77}Ge to obtain σ_m for $^{74}\text{Ge}(n, \gamma)^{75}\text{Ge}$. In order to determine the direct capture cross section σ_d to the ground state of ^{75}Ge , the relation $\sigma_d = \sigma_t - \sigma_m$ was used, because the isomeric state decays to the ground state with a branching of 99.97%. Results are given in columns 2, 3 and 4 of Table 5 for σ_t , σ_m , and σ_d for the reactions $^{74}\text{Ge}(n, \gamma)^{75}\text{Ge}$, $^{74}\text{Ge}(n, \gamma)^{75m}\text{Ge}$ and $^{74}\text{Ge}(n, \gamma)^{75d}\text{Ge}$ respectively.

Fig. 5 shows our data for σ_t in comparison to the previously existing data, evaluations and the model calculation TENDL-2013. As can be seen, our data are in fair agreement with the data of Trofimov [31] below 1 MeV and Tolstikov et al. below 3 MeV [32], while the data of Pasechnik [33] between 2.5 and 4 MeV are somewhat higher than our data and those of Tolstikov et al. Our new data almost double the energy range of the previous measurements. Below 3 MeV our data are approximately a factor of two

Table 3

Neutron capture cross-section data of ^{76}Ge obtained in the present work. Monitor cross-section σ_{mon} values for the reactions (a)–(c) given in Table 2 are taken from Refs. [23–25].

E_n (MeV)	σ_{mon} (mb)	$^{76}\text{Ge}(n, \gamma)^{77}\text{Ge}$ (mb)	$^{76}\text{Ge}(n, \gamma)^{77m}\text{Ge}$ (mb)	$^{76}\text{Ge}(n, \gamma)^{77d}\text{Ge}$ (mb)
0.38 ± 0.11	158.98 ± 5.92 (b)	6.68 ± 0.44	4.93 ± 0.36	5.75 ± 0.57
0.86 ± 0.11	166.44 ± 1.07 (a)	2.80 ± 0.22	2.94 ± 0.31	2.24 ± 0.38
1.32 ± 0.11	134.17 ± 3.22 (a)	2.30 ± 0.17	1.57 ± 0.15	2.00 ± 0.23
1.87 ± 0.11	242.66 ± 5.82 (a)	1.75 ± 0.31	1.28 ± 0.12	1.51 ± 0.33
2.77 ± 0.13	348.99 ± 8.19 (a)	1.89 ± 0.36	1.26 ± 0.25	1.65 ± 0.44
3.39 ± 0.15	336.02 ± 7.89 (a)	1.22 ± 0.22	–	–
4.39 ± 0.33	316.86 ± 7.98 (a)	0.88 ± 0.07	0.67 ± 0.08	0.75 ± 0.11
5.33 ± 0.35	335.39 ± 8.72 (a)	0.61 ± 0.09	0.37 ± 0.05	0.54 ± 0.10
6.64 ± 0.33	338.18 ± 12.01 (a)	0.44 ± 0.08	0.32 ± 0.04	0.38 ± 0.09
7.36 ± 0.29	320.78 ± 11.39 (a)	0.37 ± 0.06	0.27 ± 0.05	0.32 ± 0.07
14.81 ± 0.08	2164.39 ± 22.83 (c)	0.62 ± 0.04	–	–

Table 4

Uncertainty budget for $^{76}\text{Ge}(n, \gamma)^{77}\text{Ge}$, $^{76}\text{Ge}(n, \gamma)^{77m}\text{Ge}$, $^{74}\text{Ge}(n, \gamma)^{75}\text{Ge}$, $^{74}\text{Ge}(n, \gamma)^{75m}\text{Ge}$ and monitor reaction cross-section values.

Uncertainty	Ge (%)	Monitors (%)
Counting statistics	0.4–35	0.1–4.7
Reference cross sections		1–4.1
Detector efficiency	1–6	1–5
Source geometry and self-absorption of γ -ray	5–15	0.3–6
Half-life	<1	<0.1
γ -ray intensity	4.8–10.7	1.4–4.8
Neutron flux fluctuation	<1	<1
Lower-energy neutrons [19]	<9	<1.2

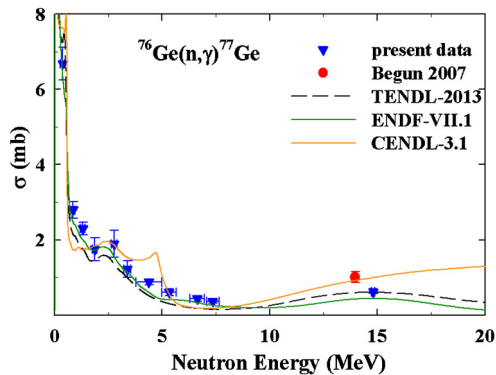


Fig. 3. (Color online.) $^{76}\text{Ge}(n, \gamma)^{77}\text{Ge}$ total cross-section data in comparison to evaluations and the model prediction TENDL-2013. The ENDF/B-VII.1 and JENDL-4.0 [28] evaluations overlap in the entire energy range. The datum of Begun et al. [26] is the only cross-section value that existed before the present measurements.

higher than the evaluations and TENDL-2013, both of which were tuned to the data of Tolstikov et al. and Trofimov. Above 4 MeV ENDF/B-VII.1 underpredicts our data by about a factor two, while TENDL-2013 is in close agreement with our data, in contradiction to lower energies.

Finally, Fig. 4 compares the neutron capture cross-section data σ_m for the isomeric 139.7 keV state of ^{75}Ge to those of the 159.7 keV isomeric state in ^{77}Ge . The former is approximately a factor of 2.5 larger than the latter.

4. Conclusion

As stated already in the introduction, the neutron slowing-down process is rather complicated. Contrary to hydrogenous materials, where MeV neutrons reach thermal energies after a relatively small number of elastic scattering and reaction processes, in “heavy” materials like germanium, neutrons undergo a large

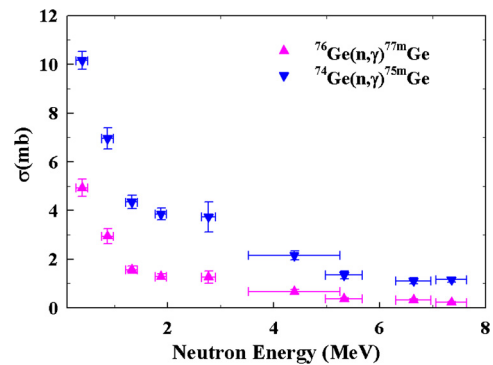


Fig. 4. (Color online.) Neutron radiative capture cross-section data to the 159.7 keV state of ^{77}Ge and the 139.7 keV state of ^{75}Ge .

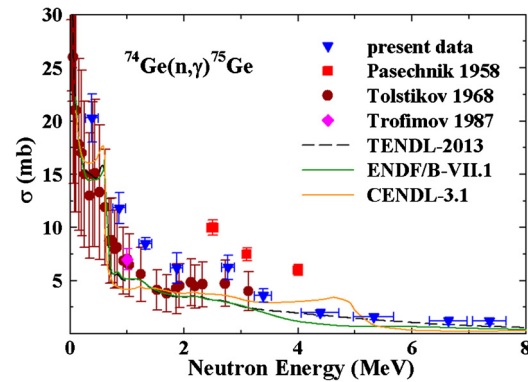


Fig. 5. (Color online.) $^{74}\text{Ge}(n, \gamma)^{75}\text{Ge}$ total cross-section data in comparison to the previously existing data and evaluations and the model prediction TENDL-2013. The ENDF/B-VII.1 and JENDL-4.0 [28] evaluations overlap in the entire energy range.

number of a variety of reaction processes during their slowing-down history. Once the neutron energy is below the (n, 2n) threshold (9.55 MeV for ^{76}Ge and 10.34 MeV for ^{74}Ge), elastic scattering and the γ -ray producing inelastic scattering reactions are the main contributors to the neutron slowing-down process. In the latter case the resulting γ rays are a potential source of background events in ^{76}Ge based $0\nu\beta\beta$ decay searches, if their energy is above 2.3 MeV. Only those γ rays can Compton scatter into the 2039 keV energy region of interest. Therefore, once the neutron energy is below approximately 2.5 MeV, inelastic scattering does not produce anymore γ rays of concern. Starting at this energy, the neutron capture reaction is the only source of γ rays that can potentially produce signals in the energy region of interest. It should also be noted that neutron transport calculations show that approximately 5% of initially 0.86 MeV neutrons incident

Table 5
Neutron capture cross-section data of ^{74}Ge obtained in the present work.

E_n (MeV)	$^{74}\text{Ge}(n, \gamma)^{75}\text{Ge}$ (mb)	$^{74}\text{Ge}(n, \gamma)^{75m}\text{Ge}$ (mb)	$^{74}\text{Ge}(n, \gamma)^{75d}\text{Ge}$ (mb)
0.38 ± 0.11	20.29 ± 2.27	10.16 ± 0.36	10.13 ± 2.30
0.86 ± 0.11	11.83 ± 1.45	6.96 ± 0.44	4.87 ± 1.06
1.32 ± 0.11	8.48 ± 0.54	4.35 ± 0.27	4.13 ± 0.57
1.87 ± 0.11	6.19 ± 1.43	3.85 ± 0.24	2.34 ± 0.88
2.77 ± 0.13	6.26 ± 1.15	3.74 ± 0.62	2.52 ± 0.88
3.39 ± 0.15	3.60 ± 0.63	–	–
4.39 ± 0.33	2.51 ± 0.42	2.16 ± 0.18	0.35 ± 0.07
5.33 ± 0.35	1.62 ± 0.28	1.35 ± 0.16	0.27 ± 0.06
6.64 ± 0.33	1.23 ± 0.34	1.11 ± 0.13	0.12 ± 0.04
7.36 ± 0.29	1.21 ± 0.27	1.16 ± 0.10	0.05 ± 0.01

on a cylinder of germanium of the isotopic composition of interest are being captured on the germanium isotopes before they are slowed down to 0.38 MeV in approximately 20 elastic scattering events. This indicates that only a small percentage of the incident neutrons reach thermal energies, where the (n, γ) cross section of ^{76}Ge and ^{74}Ge is a factor of 25 and 40, respectively, larger than that found in the present work at 0.86 MeV. Semi-qualitatively, the same results apply for shielding materials like copper or liquid argon. In realistic $0\nu\beta\beta$ setups, hydrogenous materials which convert fast neutrons very efficiently into epithermal and thermal neutrons as stated already above, are shielded by copper and lead (in Majorana) and liquid argon (in GERDA). Although mostly intended for other purposes, these materials also prevent thermal and epithermal neutrons from reaching the active detector volume. Therefore, the (n, γ) cross section in the energy range studied in the present work is of great importance for estimating neutron-induced background events in ^{76}Ge based $0\nu\beta\beta$ decay searches. They provide the necessary constraint for model calculations to accurately describe the (n, γ) cross section of ^{76}Ge above thermal energies for which previous data did not exist. The results of these calculations establish the limit on the tolerable neutron fluence to which the germanium used in $0\nu\beta\beta$ searches of ^{76}Ge can be exposed to without compromising the half-life goal of interest.

Our data also reveal that the $^{74}\text{Ge}(n, \gamma)^{75}\text{Ge}$ total radiative capture cross section is approximately a factor of 3.5 larger than that for the reaction $^{76}\text{Ge}(n, \gamma)^{77}\text{Ge}$, resulting in the finding that in the 0.4 to 14.8 MeV energy range about one third of the (n, γ) induced background in the HPGe detector used by the GERDA and Majorana Collaborations is due to ^{74}Ge , although its isotopic abundance is only 14%. Therefore, a very large scale $0\nu\beta\beta$ experiment based on natural germanium as opposed to enriched ^{76}Ge germanium, as has been discussed to reduce costs, has to be reevaluated.

Acknowledgements

We acknowledge contributions from S.W. Finch and M.E. Gooden. This work was supported partially by the U.S. Department of Energy, Office of Nuclear Physics, under Grant No. DE-FG02-97ER41033, and by the National Nuclear Security Administration under the Stewardship Science Academic Alliance Program through the U.S. Department of Energy Grant No. DE-NA0001839.

References

- [1] F.T. Avignone, S.R. Elliott, J. Engel, *Rev. Mod. Phys.* **80** (2008) 481.
- [2] M. Agostini, et al., *Phys. Rev. Lett.* **111** (2013) 122503.
- [3] N. Abgrall, et al., *Adv. High Energy Phys.* **2014** (2014) 1.
- [4] D.R. Artusa, et al., *Eur. Phys. J. C* **74** (2014) 2956.
- [5] M. Auger, et al., *Phys. Rev. Lett.* **109** (2012) 032505.
- [6] A. Gando, et al., *Phys. Rev. Lett.* **110** (2013) 062502.
- [7] R. Arnold, et al., *Eur. Phys. J. C* **70** (2010) 927.
- [8] V. Lozza, et al., *J. Phys. Conf. Ser.* **375** (2012) 042050.
- [9] Y. Toh, et al., *Phys. Rev. C, Nucl. Phys.* **87** (2013) 041304(R).
- [10] <http://www.nndc.bnl.gov>.
- [11] G. Meierhofer, P. Kudejova, L. Canella, P. Grabmayr, J. Jochum, J. Jolie, *Eur. Phys. J. A* **40** (2009) 61.
- [12] G. Meierhofer, *Phys. Rev. C, Nucl. Phys.* **81** (2010) 027603.
- [13] L. Seren, H.N. Friedlander, S.H. Turkel, *Phys. Rev.* **72** (1947) 888.
- [14] H. Pomerance, *Phys. Rev.* **88** (1952) 412.
- [15] W.S. Lyon, J.S. Eldridge, *Phys. Rev.* **107** (1957) 1056.
- [16] E. der Mateosian, M. Goldhaber, *Phys. Rev.* **108** (1957) 766.
- [17] H. Weighmann, *Z. Phys.* **167** (1962) 549.
- [18] W. Mannhart, H. Vonach, *Z. Phys.* **210** (1968) 13.
- [19] M. Bhike, W. Tornow, *Phys. Rev. C, Nucl. Phys.* **89** (2014) 031602(R).
- [20] M. Bhike, B. Fallin, W. Tornow, *Phys. Lett. B* **736** (2014) 361.
- [21] H. Liskien, A. Paulsen, *At. Data Nucl. Data Tables* **11** (1973) 569.
- [22] M. Drosog, DROSG-2000, PC database for 56 neutron reactions, documented in the IAEA report IAEA-NDS-87, Rev. 5, January 2000.
- [23] R.P. Gautam, R.K.Y. Singh, I.A. Rizvi, M. Afzal Ansari, A.K. Chaubey, S. Kailas, *Indian J. Pure Appl. Phys.* **28** (1990) 235.
- [24] A.B. Smith, S. Chiba, D.L. Smith, J.W. Meadows, P.T. Guenther, R.D. Lawson, R.J. Howerton, ANL/NDM-115 (1990).
- [25] K.I. Zolotarev, et al., INDC(NDS)-526, 2008.
- [26] S.V. Begun, O.G. Druzheruchenko, O.O. Puripirina, V.V. Tarakanov, arXiv:nucl-ex/0701039.
- [27] M.B. Chadwick, et al., *Nucl. Data Sheets* **112** (2011) 2887.
- [28] K. Shibata, et al., *Nucl. Sci. Technol.* **48** (2011) 1.
- [29] Z.G. Ge, Y.X. Zhuang, T.J. Liu, Z.S. Chang, H.C. Wu, Z.X. Zhao, H.H. Zia, in: *Proc. International Conf. on Nucl. Data for Sci. and Technol.*, Jeju Island, Korea, April 2010, p. 26.
- [30] A.J. Koning, D. Rochman, *Nucl. Data Sheets* **113** (2012) 2841.
- [31] Yu.N. Trofimov, in: *Int. Conf. on Neutron Physics*, Kiev, 14–18 Sep. 1987, vol. 3, p. 331.
- [32] V.A. Tolstikov, V.P. Koroleva, V.E. Kolesov, A.G. Dovbenko, *At. Energ.* **23** (1967) 566.
- [33] M.V. Pasechnik, et al. in: *Internat. At. Energ. Conf. Geneva*, vol. 15, 1958, p. 18.